



## OPEN ACCESS

## EDITED BY

Joseph E. Borovsky,  
Space Science Institute, United States

## REVIEWED BY

Larry Kepko,  
Goddard Space Flight Center (NASA),  
United States

## \*CORRESPONDENCE

Larry R. Lyons,  
✉ larry@atmos.ucla.edu

## SPECIALTY SECTION

This article was submitted to Space Physics, a section of the journal Frontiers in Astronomy and Space Sciences

RECEIVED 18 January 2023

ACCEPTED 16 March 2023

PUBLISHED 27 April 2023

## CITATION

Lyons LR, Nishimura Y, Liu J, Zou Y, Bristow WA, Yadav S, Donovan E, Nishitani N, Shiokawa K and Hosokawa K (2023), Unsolved problems: Mesoscale polar cap flow channels' structure, propagation, and effects on space weather disturbances.  
*Front. Astron. Space Sci.* 10:1147531.  
doi: 10.3389/fspas.2023.1147531

## COPYRIGHT

© 2023 Lyons, Nishimura, Liu, Zou, Bristow, Yadav, Donovan, Nishitani, Shiokawa and Hosokawa. This is an open-access article distributed under the terms of the [Creative Commons Attribution License \(CC BY\)](https://creativecommons.org/licenses/by/4.0/). The use, distribution or reproduction in other forums is permitted, provided the original author(s) and the copyright owner(s) are credited and that the original publication in this journal is cited, in accordance with accepted academic practice. No use, distribution or reproduction is permitted which does not comply with these terms.

# Unsolved problems: Mesoscale polar cap flow channels' structure, propagation, and effects on space weather disturbances

Larry R. Lyons<sup>1\*</sup>, Yukitoshi Nishimura<sup>2</sup>, Jiang Liu<sup>1,3</sup>, Ying Zou<sup>4</sup>, William A. Bristow<sup>5</sup>, Sneha Yadav<sup>1</sup>, Eric Donovan<sup>6</sup>, Nozomu Nishitani<sup>7</sup>, Kazuo Shiokawa<sup>7</sup> and Keisuke Hosokawa<sup>8</sup>

<sup>1</sup>Department of Atmospheric and Oceanic Sciences, University of California, Los Angeles, CA, United States, <sup>2</sup>Department of Electrical and Computer Engineering, Center for Space Physics, Boston University, Boston, MA, United States, <sup>3</sup>Department of Earth, Planetary and Space Sciences, University of California, Los Angeles, CA, United States, <sup>4</sup>Department of Space Science, University of Alabama in Huntsville, Huntsville, AL, United States, <sup>5</sup>Department of Meteorology and Atmospheric Science, The Pennsylvania State University, State College, PA, United States, <sup>6</sup>Department of Physics and Astronomy, University of Calgary, Calgary, AB, Canada, <sup>7</sup>Institute for Space-Earth Environmental Research, Nagoya University, Nagoya, Aichi, Japan, <sup>8</sup>Graduate School of Communication Engineering and Informatics, University of Electro-Communications, Tokyo, Chofu, Japan

Dynamic mesoscale flow structures move across the open field line regions of the polar caps and then enter the nightside plasma sheet where they can cause important space weather disturbances, such as streamers, substorms, and omega bands. The polar cap structures have long durations (apparently at least  $\sim 1\frac{1}{2}$  to 2 h), but their connections to disturbances have received little attention. Hence, it will be important to uncover what causes these flow enhancement channels, how they map to the magnetospheric and magnetosheath structures, and what controls their propagation across the polar cap and their dynamic effects after reaching the nightside auroral oval. The examples presented here use 630-nm auroral and radar observations and indicate that the motion of flow channels could be critical for determining when and where a particular disturbance within the nightside auroral oval will be triggered, and this could be included for full understanding of flow channel connections to disturbances. Also, it is important to determine how polar cap flow channels lead to flow channels within the auroral oval, i.e., the plasma sheet, and determine the conditions along nightside oval/plasma sheet field lines that interact with an incoming polar cap flow channel to cause a particular disturbance. It will also be interesting to consider the generality of geomagnetic disturbances being related to connections with incoming polar cap flow channels, including the location, time, and type of disturbances, and whether the duration and expansion of disturbances are related to flow channel duration and to multiple flow channels.

## KEYWORDS

polar cap, space weather, auroral streamers, substorms, flow channels, geomagnetic disturbances, streamers, omega bands

## 1 Introduction

Recent evidence indicates that the magnetosphere–ionosphere system is frequently driven by dynamic mesoscale flow structures (see Chapters in [Nishimura et al., 2022](#), and references therein) that are first observed near the dayside cusps, move across the open field line regions of the polar caps, and then enter the plasma sheet, where they lead to a number space weather disturbances ([Lyons et al., 2016](#), and references therein). It is important to uncover the features of these channels of enhanced flow, i.e., their structure, how they propagate across the polar cap, and what controls their dynamic effects after reaching the nightside plasma sheet. On the dayside, ionospheric flow channels emanate from regions of localized reconnection along the open–closed field line boundary and are associated with poleward moving auroral forms (PMAFs) that track flow channels as they move poleward into the polar cap (e.g., [Sandholt et al., 2002](#)). The electron precipitation that produces PMAFs leads to areas of high-density F-region plasma called polar cap airglow patches that continue propagating poleward after PMAF decay ([Carlson et al., 2006](#); [Lorentzen et al., 2010](#)). They continue to mark flow channels as they propagate across the polar cap ([Nishimura et al., 2014](#); [Zou et al., 2015](#); [Wang et al., 2016](#)). When they reach the nightside auroral oval, it is observed that the flow channels in the polar cap lead to flow channels within the oval ([de la Beaujardière et al., 1994](#); [Lyons et al., 2011](#); [Pitkänen et al., 2013](#)), which form auroral poleward boundary intensifications (PBIs) ([Lorentzen et al., 2004](#); [Nishimura et al., 2013](#); [Zou et al., 2014](#)). However, the physics of the interaction of flow channels along the nightside open–closed field line boundary remains to be investigated, as well as does how many, and which, auroral oval flow channels result from this interaction. Some PBIs subsequently extend toward the equator as auroral streamers, indicating an equatorward extension of the flow channels within the oval. Auroral streamers and their associated flow channels represent a common geomagnetic disturbance, and the observations of auroral streamer indicate that some of these flow channels cause major geomagnetic disturbances, such as substorms ([Nishimura et al., 2010](#)) and dawnside omega bands ([Henderson et al., 2002](#); [Liu et al., 2018](#)).

Using simultaneous observations of the dayside, polar cap, and nightside polar region by all-sky imagers (ASIs), SuperDARN radars, and a Defense Meteorological Satellite Program (DMSP) satellite, [Nishimura et al. \(2014\)](#) observed the nearly continuous progression of a PMAF becoming a polar cap patch and then propagating across the polar cap from the dayside auroral region toward the nightside auroral oval. The patch was associated with a narrow flow channel when it reached the nightside polar cap, indicating that fast mesoscale flows initiating on the dayside transported the enhanced plasma density over a limited longitude range toward the nightside auroral oval. As the flow channel and patch reached the nightside auroral poleward boundary, PBIs developed. It is interesting to note that this flow channel was tracked across the polar cap for ~90 min before it led to PBIs. A similar traversal from the dayside to the nightside auroral oval (taking ~110 min) was shown for polar cap patches by [Zhang et al. \(2013\)](#), which, based on patches being carried by polar cap flow channels, can be regarded as an observation of a similar traversal of a flow channel from the dayside to the nightside plasma sheet.

If generally true, the concept that flow channels leading to major space weather disturbances on the nightside propagate within the polar cap before they lead to a disturbance would likely be critical for deep understanding of the causes of space weather. Despite this potential importance, the topic has received very less attention. [Nishimura & Lyons \(2016\)](#) considered one possibility of how this process might be driven. They showed that, based on an MHD simulation of the response to an interplanetary magnetic field (IMF) discontinuity, localized flow channels can propagate tailward across the lobe and drive localized magnetotail reconnection when they reach the outer boundary of the nightside plasma sheet and that the cross-tail width of this reconnection and resulting plasma sheet flow channels and dipolarization fronts are related to the width of the inflow from the lobe. Certainly, this subject deserves much additional attention. In the following sections, we put forward a further aspect of this crucial coupling of polar cap flow channels to space weather disturbances (to be included in further considerations) and conclude with critical questions about polar cap flow channels and the relation to space weather.

When observed on a large scale, polar cap convection varies substantially from purely anti-sunward flow in response to the y-component of the IMF ([Mansurov, 1970](#); [Stern, 1973](#); [Svalgaard, 1973](#); [Reiff and Burch, 1985](#)), giving a substantial azimuthal component to flow within the nightside polar cap, that is, from dawn to dusk (dusk-to-dawn) for IMF  $B_y > 0$  ( $< 0$ ). Flow channels are embedded in this large-scale convection and contribute to total convection, an individual channel contributing ~10%–40% of the cross-polar cap potential drop and having orientation that tends to agree with that expected from the orientation of the IMF by [Zou et al. \(2015\)](#). It is thus reasonable to consider that flow channels also move across the polar cap with an azimuthal motion that reflects this IMF by dependence. While there is not enough capability to measure polar cap flow to directly detect the motion of flow channels, the flows can be tracked with the red line (630 nm) all-sky-imager (ASI) data ([Carlson, 1990](#)). This allows detecting the weak emissions from polar-cap patches as well as detecting the weak emissions (compared to auroral oval arcs) of polar cap arcs. In addition to patches, whose motion traces that of flow channels ([Zou et al., 2015](#)), polar cap arcs are located toward the edge of a localized flow channel ([Robinson et al., 1987](#); [Valladares and Carlson, 1991](#); [Koustov et al., 2009](#)) and thus, their azimuthal motion traces that of flow channels. In the following sections, we show a by dependent azimuthal motion of polar cap arcs and their associated flow channels over nearly 2-h periods and that these flow channels are the dominant driver of geomagnetic activity as observed by auroral oval substorm activity and ground magnetic depressions.

## 2 2013 March 9; IMF $B_y > 0$ example

[Figure 1](#) shows selected mosaics of images for 0704–0920 UT on 9 March 2013, from the 630-nm ASI at Resolute Bay (83° magnetic latitude), which is part of the Optical Mesosphere Thermosphere Imager (OMTI) network ([Shiokawa et al., 1999](#)) of 630-nm ASIs, and the lower-latitude THEMIS white light ASIs covering North America ([Mende et al., 2008](#)). [Supplementary Movie S1](#) shows a recording of the mosaics every 2 min over the full-time interval of interest. The IMF  $B_y$  was mostly ~3–4 nT, and  $B_z$  varied between

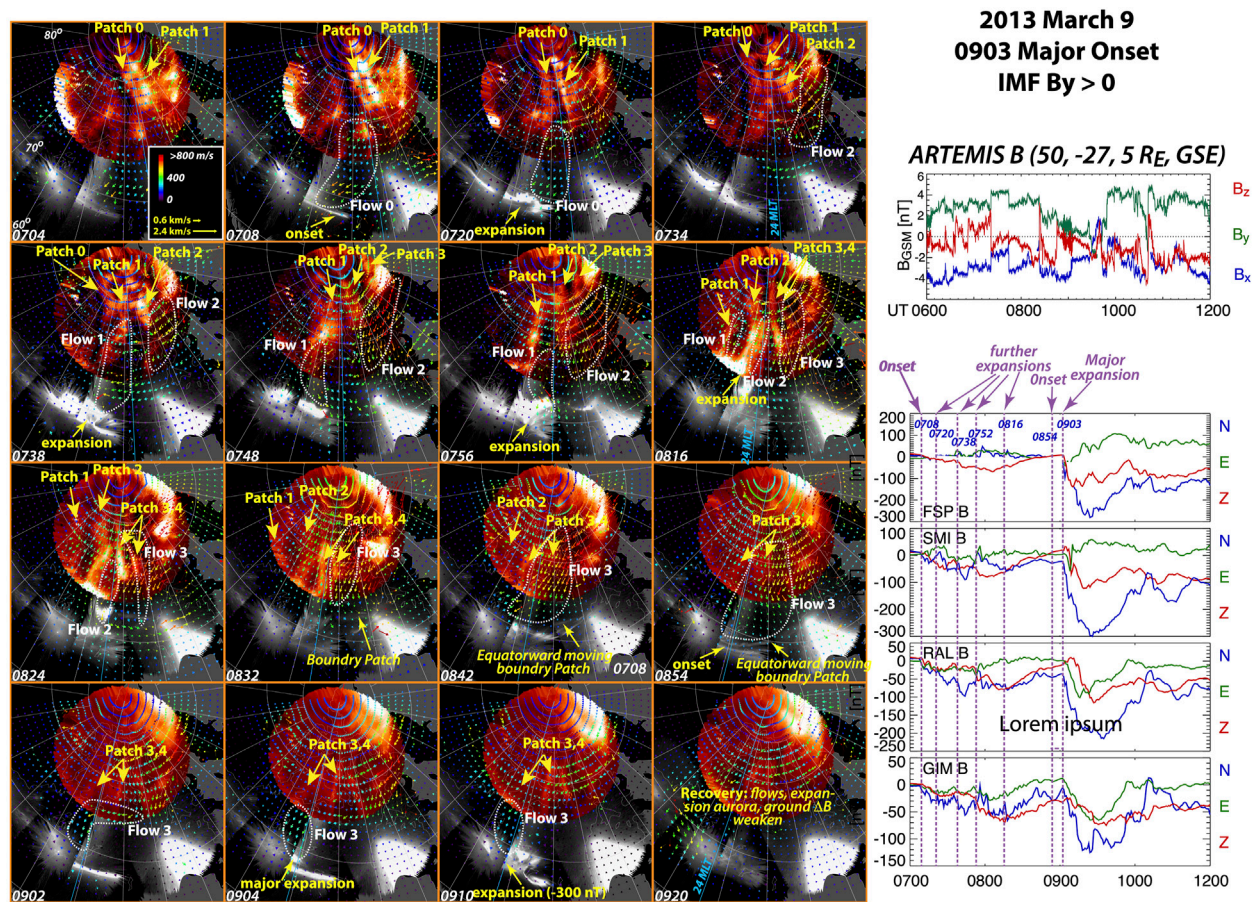


**FIGURE 1** Selected mosaics of images for 0704–0920 UT on 9 March 2013 from the REGO 630 nm ASI at Resolute Bay (83° magnetic latitude) and the lower-latitude THEMIS while light ASIs cover North America. [Supplementary Movie S1](#) shows a movie of the mosaics every 2 min over the full-time interval of interest. Overlaid on the mosaics are two-dimensional flow vectors obtained from all available SuperDARN radar echoes as described in the text. The IMF as measured by the closest available monitor, ARTEMIS B, and ground magnetometer measurements in the vicinity of the auroral disturbance are shown along the right side of the figure.

~ -2 and 1 nT. The 630-nm ASI observations show several narrow optical forms extending toward the equator across the field-of-view (FOV) from near the magnetic pole toward the nightside auroral oval, which is observed primarily by the THEMIS ASIs. These relatively diffuse emissions resemble polar cap patches, and five of them are labeled as Patch 0–4 in the figure. These patches can be seen to move from the dawnside to the duskside of the polar cap during their anti-sunward motion, crossing magnetic midnight (identified with a blue meridional line), with this duskward motion across the polar cap being particularly clear in [Supplementary Movie S1](#).

Figure 1 and [Supplementary Movie S1](#) show that two-dimensional flow vectors obtained from all available SuperDARN radar echoes are overlaid on the mosaics, using the divergence-free condition (Bristow et al., 2016; Bristow et al., 2022). Here, the divergence-free flow pattern was obtained from the line-of-sight (LOS) SuperDARN velocity adopted from the Spherical Elementary Current Systems (SECS) (Amm et al., 2010) technique and gives a divergence-free solution over a 1° latitude and 3° longitude grid. No background statistical convection model was used to avoid the

influence of prescribed background flows and emphasize the continuity of observed flow channels. Heavier arrows represent the flow vectors obtained in regions of radar echoes, and thin arrows represent the flows in regions without echoes. Since there is no background convection model, the flows here are only meaningful in and near regions of echoes, unlike in Bristow et al. (2016) and Bristow et al. (2022). Regions of enhanced, approximately equatorward, flow that we identify as flow channels associated with one of the identified polar cap patches are roughly encircled by white dashed curves.

These flow channels appear to substantially affect auroral dynamics as they are swept from east to west across the nightside. As Patch 0 is swept by from east to west, the flow channel associated with Patch 0 moves toward the equatorward boundary of the auroral oval at 0708 UT (relative to what was seen at 0704 and 0706 UT). This is the time of an east–west aligned auroral arc brightening near the equatorward boundary of the auroral oval, which we identify as a substorm onset. As can be seen in the 0720 UT panel, the substorm auroral brightening then expanded poleward and azimuthally after onset. Such flows leading to onsets

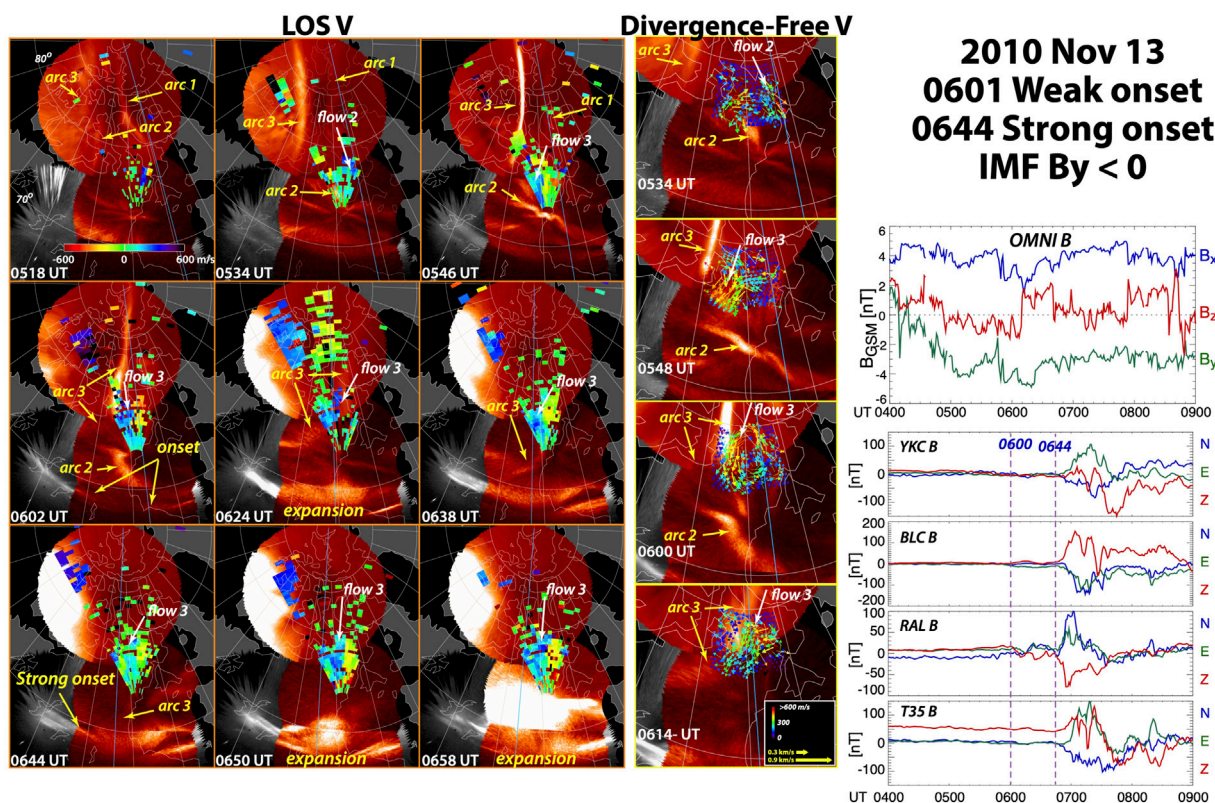


FIGURE 2

Selected mosaics of images for 0518–0614 UT on 13 November 2010 as in Figure 1. Supplementary Movie S3 shows a movie of the mosaics every 2 min over the full-time interval of interest displaying more of the THEMIS ASI imagers FOVs than in Figure 2. Overlaid on the mosaics are LOS flows obtained from all available SuperDARN radar echoes. Images with two-dimensional flows are shown in the column to the right of the images with LOS flows for times when the two-dimensional flow was of sufficient quality to discern a flow channel and its relation to a polar cap arc. The IMF from NASA OMNIWeb and ground magnetometer measurements in the vicinity of the auroral disturbance are shown along the right side of the figure.

and their azimuthal expansion have been previously identified using the Bristow et al. (2016) two-dimensional flows (Lyons et al., 2022). Flows to the onset decreased as Patch 0 moved further westward, and further expansion was temporarily reduced, as seen in the 0734 UT panel. However, soon thereafter, Patch 1 moved westward to the longitude of the expansion-phase auroral bulge, and the flow channel with this patch impinged on the bulge as seen in the 0738 UT panel and Supplementary Movie S1 from 0736 to 0756 UT, leading to further poleward and azimuthal expansion of the expansion phase bulge. This is only a modest substorm with peak magnetic northward N component magnetic depression of ~100 nT as seen in the SMI and RAL magnetograms in the lower right portion of Figure 1, the peak detected depression being ~150 nT at FCC (not included in Figure 2). A further intensification of this auroral bulge occurred, as seen in the 0816 UT panel, as Patch 2 and its associated flow reached the longitude of the bulge. It is interesting to note that a direct connection can be seen between Patch 2 and the bulge in the 630-nm images from ~0812 to 0826 UT as Patch 2 swept westward across the bulge. Flows to the bulge decreased as Patch 2 swept westward, and expansion-phase auroral activity decreased.

With the occurrence of the aforementioned activity, Patches 3 and 4 moved westward from the dawnside edge of the 630-nm FOV. The flow channel associated with these patches first becomes clear at 0806 UT in the movie and is identified as Flow 3 in the

0816 UT panel of Figure 1. Its equatorward edge is initially seen above 75° latitude and then gradually moved equatorward. As it moved equatorward, an arc appearing along the oval poleward boundary, that is, first visible in Supplementary Movie S1 at 0830 UT was pushed equatorward until it reached very near the equatorward boundary of the auroral oval and to an arc brightening that demarcates an onset at 0854 UT. As flow channel 3 continued to flow into the onset region, a major substorm poleward and azimuthal expansion can be identified at 0904 UT, leading to magnetic depressions of 300 nT. Visible polar cap patches and flow channels decreased by 0920 UT, auroral activity decreased, and the stronger magnetic depressions at FSP and SMI decreased.

We have three polar-orbiting DMSP passes over the polar caps during this event (Supplementary File S2), two over the southern hemisphere, and one over the northern hemisphere. Auroral images taken from horizon-to-horizon scans in the direction normal to the spacecraft trajectory from the two southern hemisphere passes are shown in the lower panels (DMSP 16 and 17). The images show the main auroral oval, but are not sufficiently sensitive to show the polar cap patches. As expected for IMF  $B_y > 0$ , anti-sunward convection (second panel) is much stronger on the dusk/dawnside in the southern/northern hemisphere (DMSP 16,17/15) of the polar cap region (MLAT >73°) because of the anti-sunward flow. It is of particular interest that, as indicated by shadings in the figure,

considerable structure appears in the region of strong anti-sunward flows. The localized enhanced anti-sunward flows are likely responsible for carrying polar cap patches from the dayside toward the nightside, and the related structuring of the cross-track magnetic field (top panels) likely reflects associated magnetic field aligned currents.

### 3 2010 November 13; IMF By < 0 example

Figure 2 shows selected mosaics of images for 0518–0614 UT on 2010 November 13 as in Figure 1. Supplementary Movie S3 shows a recording of the mosaics every 2 min over the full-time interval of interest, displaying more of the THEMIS ASI imagers FOVs than in Figure 2. The red line ASIs at latitudes below the Resolute Bay ASI are from the Red-line Emission Geospace Observatory (REGO) (Gillies et al., 2017) (<https://www.ucalgary.ca/aurora/projects/rego>) ASIs at Rankin Inlet and Taloyoak. Overlaid on the mosaics in Figure 2 and Supplementary Movie S3 are the line-of-sight (LOS) flow obtained from all available SuperDARN radar echoes. Images with two-dimensional flows are shown in the column to the right of the images with LOS flows for times when the two-dimensional flow was of sufficient quality to discern a flow channel and its relation to a polar cap arc. The IMF  $B_y$  was mostly  $\sim -3$  to  $-4$  nT, and  $B_z$  varied between  $\sim -1$  and 1 nT. As can be seen in Figure 2 and Supplementary Movie S3, polar cap arcs sweep from west to east in this case, as expected from the northern hemisphere flow pattern for  $B_y < 0$ .

Three polar cap arcs are identified in the first (0518 UT) panel. The eastern-most arc (arc 1) moved eastward and then slowly disappeared. The next arc to the west, arc 2, also moved eastward and extended equatorward toward the auroral oval. The LOS and vector flows in the 0634 UT panels indicate a flow channel adjacent to arc 2. As this arc extended equatorward, it (more accurately, the associated flow channel) led to an auroral onset near its point of contact with the auroral oval, as can be seen at 0600 UT in Supplementary Movie S3 and identified in the 0602 UT panel of Figure 2. Limited expansion of auroral activity was observed after this onset and continued until  $\sim 0630$  UT. This is identified in the 0624 UT panel of Figure 2 and seen more clearly in the THEMIS ASI images in the movie, where more of the THEMIS ASIs' FOVs are displayed at lower oval latitudes than that shown in Figure 2. Due to the limited poleward expansion and weak ground magnetic perturbations, this onset would generally be called a pseudo-breakup.

Arc 3 is traced moving westward and extending equatorward as shown in Figure 2 for nearly 1½ hours, and a flow channel was seen adjacent to the arc starting at 0546 UT when the arc approached the region of SuperDARN radar echoes. It is of particular interest that, as the arc extended equatorward toward the auroral oval, its equatorward portion bent strongly toward the west, as can be seen in the images in Figure 2 and Supplementary Movie S3 starting at 0600 UT. The equatorward-most portion of the arc became almost parallel to the oval, and as this approximately east–west aligned segment of the arc moved equatorward and contacted the auroral oval, it (more accurately, the associated flow channel) leads to an onset at 0644 UT that extended over

several hours in MLT, and the bulge auroral activity subsequently expanded poleward by several degrees in latitude. The ground magnetic perturbations with this substorm were moderate, peaking a little over 100 nT.

## 4 Perspective

We argue here that understanding of flow channels as they propagate across the polar cap and reach the nightside auroral oval should be a critical goal to understand what controls space weather. The limited examples published previously, and the two examples presented here, indicate that these flow channels move within the polar cap for at least 1½–2 h before they impact the nightside oval and lead to dominant geomagnetic disturbances, in particular PBIs, streamers, substorm, and omega bands. Tracking of flow channels within the polar cap can be carried out with radars, density and optical signatures of polar cap patches, and observations of polar cap arcs, which can be seen in 630-nm emissions from ground-based ASIs. The examples presented here suggest that, as the flow channels propagated anti-sunward within the polar cap, their azimuthal motion may be significantly controlled by the IMF  $B_y$ -dependent large-scale convection, and this motion could be critical for determining when and where a particular disturbance will be triggered. Critical questions about polar cap flow channels and the relation to space weather include the following:

1. What controls the propagation of flow channels within the polar cap and when and how do enhanced flows extend across, or move across, the polar cap and reach the nightside auroral oval boundary? This includes what conditions control the mapping of structures from the magnetosheath and magnetosphere to the polar cap ionosphere and what controls the mapping spatial and time scales.
2. When and how does localized reconnection occur and bring enhanced flow channels, and lobe and polar cap ionospheric plasma, into the auroral oval/plasma sheet?
3. How many, and which, auroral oval flow channels result from the impact of polar cap flow channels on the poleward boundary of the auroral oval?
4. What is the role of new plasma brought into the plasma sheet from the polar caps by the localized reconnection at the polar cap boundary?
5. Under what conditions do the flow channels propagate a significant distance equatorward/earthward within the oval/plasma sheet?
6. Under what conditions do flow channels from the polar cap lead to disturbances such as substorms, streamers, and dawnside omega bands?
7. How is the azimuthal motion of flow channels related to the time and location of disturbances, including the driving of multiple disturbances by the same flow channel?
8. How do the conditions for leading to a disturbance depend upon the evolution of plasma sheet conditions while a flow channel moves within the polar cap? Although we do not have statistics on polar cap flow propagation times, the time scale for flow channels within the polar cap appears to be much longer than for conditions to change within the nightside plasma sheet.

For example, the growth phase of substorm is typically much less than an hour.

9. All the disturbances during the two time intervals considered here are related to incoming polar cap flow channels. How general is this relationship?
10. What is the role of the duration of a polar cap flow channel, and multiple flow channels, in the temporal and spatial evolution of disturbances?

## Data availability statement

Publicly available datasets were analyzed in this study. These data can be found here: Optical Mesosphere Thermosphere Imagers (OMTI) network data are provided by the ERG Science Center at <https://ergsc.isee.nagoya-u.ac.jp/index.shtml.en>. REGO data were obtained from <https://www.ucalgary.ca/aurora/projects/rego>. SuperDARN data were obtained from: <http://vt.superdarn.org/tiki-index.php?page=Data+Access>. The solar wind and geomagnetic index data are provided by the NASA OMNIWeb (<http://omniweb.gsfc.nasa.gov/>), and the ground magnetometer data were obtained from the SuperMAG website, <https://supermag.jhuapl.edu/>, that uses processing described in Gjerloev (2012). Auroral images of the Special Sensor Ultraviolet Spectrographic Imager onboard polar-orbiting DMSP spacecraft were obtained from [https://ssusi.jhuapl.edu/gal\\_AUR](https://ssusi.jhuapl.edu/gal_AUR). The DMSP measurements of precipitating particles, plasma flow, and magnetic field were obtained from the Madrigal database (<http://millstonehill.haystack.mit.edu/index.html>). The THEMIS ASI AND IMF data from were obtained from <http://themis.ssl.berkeley.edu/themisdata/>.

## Author contributions

LL, YN, and YZ contributed to the approach for this study, and JL contributed to analysis of interplanetary and ground-based magnetometer data. WB and YN contributed to the novel approach for determining two-dimensional flow vectors. ED, NN, and KS contributed to the data and its presentation, LL wrote the first draft of the manuscript, and YN, YZ, JL, SY, and WB contributed to the text.

## References

- Amm, O., Grocott, A., Lester, M., and Yeoman, T. K. (2010). Local determination of ionospheric plasma convection from coherent scatter radar data using the SECS technique. *J. Geophys. Res. Space Phys.* 115 (A3). doi:10.1029/2009JA014832
- Bristow, W. A., Hampton, D. L., and Otto, A. (2016). High-spatial-resolution velocity measurements derived using Local Divergence-Free Fitting of SuperDARN observations. *J. Geophys. Res. Space Phys.* 121 (2), 1349–1361. doi:10.1002/2015JA021862
- Bristow, W. A., Lyons, L. R., Nishimura, Y., Shepherd, S. G., and Donovan, E. F. (2022). High-latitude plasma convection based on SuperDARN observations and the locally divergence free criterion. *J. Geophys. Res. Space Phys.* 127 (12), e2022JA030883. doi:10.1029/2022JA030883
- Carlson, H. C., Jr. (1990). Dynamics of the quiet polar cap. *J. geomagnetism Geoelectr.* 42 (6), 697–710. doi:10.5636/jgg.42.697
- Carlson, H. C., Moen, J., Oksavik, K., Nielsen, C. P., McCrea, I. W., Pedersen, T. R., et al. (2006). Direct observations of injection events of subauroral plasma into the polar cap. *Geophys. Res. Lett.* 33 (5), L05103. doi:10.1029/2005GL025230
- de la Beaujardière, O., Lyons, L. R., Ruohoniemi, J. M., Friis-Christensen, E., Danielsen, C., Rich, F. J., et al. (1994). Quiet-time intensifications along the poleward auroral boundary near midnight. *J. Geophys. Res.* 99 (A1), 287–298. doi:10.1029/93JA01947
- Gillies, D. M., Knudsen, D., Donovan, E., Jackel, B., Gillies, R., and Spanswick, E. (2017). Identifying the 630 nm auroral arc emission height: A comparison of the triangulation, fac profile, and electron density methods. *J. Geophys. Res. Space Phys.* 122 (8), 8181–8197. doi:10.1002/2016JA023758
- Gjerloev, J. W. (2012). The SuperMAG data processing technique. *J. Geophys. Res. Space Phys.* 117 (A9), A09213. doi:10.1029/2012JA017683
- Henderson, M. G. L., Kepko, H. E., Spence, M., Connors, J. B., Sigwarth, L. A. F., and Singer, H. J. (2002). "The evolution of north-south aligned auroral forms into auroral torch structures: The generation of omega bands and ps6 pulsations via flow bursts," in *Sixth international conference on substorms*. Editor R. M. Winglee (Seattle: The University of Washington), 169–174.
- Koustov, A. V., St.-Maurice, J. P., Sofko, G. J., Andre, D., MacDougall, J. W., Hairston, M. R., et al. (2009). Three-way validation of the Rankin Inlet PolarDARN radar velocity measurements. *Radio Sci.* 44 (4). doi:10.1029/2008RS004045
- Liu, J., Lyons, L. R., Archer, W. E., Gallardo-Lacourt, B., Nishimura, Y., Zou, Y., et al. (2018). Flow shears at the poleward boundary of omega bands observed during conjunctions of swarm and THEMIS ASI. *Geophys. Res. Lett.* 45 (3), 1218–1227. doi:10.1002/2017GL076485
- Lorentzen, D. A., Moen, J., Oksavik, K., Sigernes, F., Saito, Y., and Johnsen, M. G. (2010). *In situ* measurement of a newly created polar cap patch. *J. Geophys. Res. Space Phys.* 115 (A12), A12323. doi:10.1029/2010JA015710

## Funding

Work at UCLA has been supported by NSF grant 1907483, NASA grants 80NSSC20K1314 and 80NSSC22K0749, and AFOSR FA9559-16-1-0364, at Boston University by AFOSR FA9559-16-1-0364, NASA NNX17AL22G, NSF AGS-1737823, and AFOSR FA9550-15-1-0179. SuperDARN work at Penn State was supported by AFOSR FA9559-16-1-0364. SuperDARN operations and research at Pennsylvania State University are supported under NSF grants PLR-1443504 from the Office of Polar Programs, and AGS-1934419 from the Geospace Section of NSF Division of Atmospheric and Geospace Sciences. SuperDARN is a collection of radars funded by national scientific funding agencies of Australia, Canada, China, France, Italy, Japan, Norway, South Africa, the United Kingdom, and the United States of America.

## Conflict of interest

The authors declare that the research was conducted in the absence of any commercial or financial relationships that could be construed as a potential conflict of interest.

## Publisher's note

All claims expressed in this article are solely those of the authors and do not necessarily represent those of their affiliated organizations, or those of the publisher, the editors, and the reviewers. Any product that may be evaluated in this article, or claim that may be made by its manufacturer, is not guaranteed or endorsed by the publisher.

## Supplementary material

The Supplementary Material for this article can be found online at: <https://www.frontiersin.org/articles/10.3389/fspas.2023.1147531/full#supplementary-material>

- Lorentzen, D. A., Shumilov, N., and Moen, J. (2004). Drifting airglow patches in relation to tail reconnection. *Geophys. Res. Lett.* 31 (2). doi:10.1029/2003GL017785
- Lyons, L. R., Nishimura, Y., Kim, H. J., Donovan, E., Angelopoulos, V., Sofko, G., et al. (2011). Possible connection of polar cap flows to pre- and post-substorm onset PBIs and streamers. *J. Geophys. Res.* 116, 14. doi:10.1029/2011ja016850
- Lyons, L. R., Nishimura, Y., Liu, J., Bristow, W. A., Zou, Y., and Donovan, E. F. (2022). Verification of substorm onset from intruding flow channels with high-resolution SuperDARN radar flow maps. *J. Geophys. Res. Space Phys.* 127 (8), e2022JA030723. doi:10.1029/2022JA030723
- Lyons, L. R., Nishimura, Y., and Zou, Y. (2016). Unsolved problems: Mesoscale polar cap flow channels' structure, propagation, and effects on space weather disturbances. *J. Geophys. Res. Space Phys.* 121 (4), 3347–3352. doi:10.1002/2016JA022437
- Mansurov, S. M. (1970). New evidence of a relationship between magnetic fields in space and on earth. *Geomagnetism Aeronomy* 9, 622.
- Mende, S. B., Harris, S. E., Frey, H. U., Angelopoulos, V., Russell, C. T., Donovan, E., et al. (2008). The THEMIS array of ground-based observatories for the study of auroral substorms. *Space Sci. Rev.* 141 (1–4), 357–387. doi:10.1007/s11214-008-9380-x
- Y. Nishimura, O. Verkhoglyadova, Y. Deng, and S. -R. Zhang (Editors) (2022). 'Front matter', in *cross-scale coupling and energy transfer in the magnetosphere-ionosphere-thermosphere system* (Elsevier), i–ii. doi:10.1016/B978-0-12-821366-7.09988-1
- Nishimura, Y., and Lyons, L. R. (2016). Localized reconnection in the magnetotail driven by lobe flow channels: Global MHD simulation. *J. Geophys. Res. Space Phys.* 121 (2), 1327–1338. doi:10.1002/2015JA022128
- Nishimura, Y., Lyons, L. R., Shiokawa, K., Angelopoulos, V., Donovan, E. F., and Mende, S. B. (2013). Substorm onset and expansion phase intensification precursors seen in polar cap patches and arcs. *J. Geophys. Res. Space Phys.* 118 (5), 2034–2042. doi:10.1002/jgra.50279
- Nishimura, Y., Lyons, L. R., Zou, Y., Oksavik, K., Moen, J. I., Clausen, L. B., et al. (2014). Day-night coupling by a localized flow channel visualized by polar cap patch propagation. *Geophys. Res. Lett.* 41 (11), 3701–3709. doi:10.1002/2014GL060301
- Nishimura, Y., Lyons, L., Zou, S., Angelopoulos, V., and Mende, S. (2010). Substorm triggering by new plasma intrusion: THEMIS all-sky imager observations. *J. Geophys. Res.* 115 (A7). doi:10.1029/2009JA015166
- Pitkänen, T., Aikio, A. T., and Juusola, L. (2013). Observations of polar cap flow channel and plasma sheet flow bursts during substorm expansion. *J. Geophys. Res. Space Phys.* 118 (2), 774–784. doi:10.1002/jgra.50119
- Reiff, P. H., and Burch, J. L. (1985). IMF by-dependent plasma flow and birkeland currents in the dayside magnetosphere: 2. A global model for northward and southward IMF. *J. Geophys. Res. Space Phys.* 90 (A2), 1595–1609. doi:10.1029/JA090iA02p01595
- Robinson, R. M., Vondrak, R. R., Miller, K., Dabbs, T., and Hardy, D. (1987). On calculating ionospheric conductances from the flux and energy of precipitating electrons. *J. Geophys. Res.* 92 (A3), 2565. doi:10.1029/JA092iA03p02565
- Sandholt, P. E., Carlson, H. C. and Egeland, A. (Editors) (2002). *Dayside and polar cap aurora* (Dordrecht: Springer Netherlands (Astrophysics and Space Science Library) (Accessed September 26, 2022). doi:10.1007/0-306-47969-9\_1
- Shiokawa, K., Katoh, Y., Satoh, M., Ejiri, M. K., Ogawa, T., Nakamura, T., et al. (1999). Development of optical Mesosphere Thermosphere imagers (OMTI). *Earth, Planets, Space* 51, 887–896. doi:10.1186/bf03353247
- Stern, D. P. (1973). A study of the electric field in an open magnetospheric model. *J. Geophys. Res.* 78 (31), 7292–7305. doi:10.1029/JA078i031p07292
- Svalgaard, L. (1973). Polar cap magnetic variations and their relationship with the interplanetary magnetic sector structure. *J. Geophys. Res.* 78 (13), 2064–2078. doi:10.1029/JA078i013p02064
- Valladares, C. E., and Carlson, H. C. (1991). The electrodynamic, thermal, and energetic character of intense Sun-aligned arcs in the polar cap. *J. Geophys. Res. Space Phys.* 96 (A2), 1379–1400. doi:10.1029/90JA01765
- Wang, B., Nishimura, Y., Lyons, L. R., Zou, Y., Carlson, H. C., Frey, H. U., et al. (2016). Analysis of close conjunctions between dayside polar cap airglow patches and flow channels by all-sky imager and DMSP. *Earth, Planets Space* 68 (1), 150. doi:10.1186/s40623-016-0524-z
- Zhang, Q.-H., Zhang, B. C., Lockwood, M., Hu, H. Q., Moen, J., Ruohoniemi, J. M., et al. (2013). Direct observations of the evolution of polar cap ionization patches. *Science* 339 (6127), 1597–1600. doi:10.1126/science.1231487
- Zou, Y., Nishimura, Y., Lyons, L. R., Donovan, E. F., Ruohoniemi, J. M., Nishitani, N., et al. (2014). Statistical relationships between enhanced polar cap flows and PBIs. *J. Geophys. Res. Space Phys.* 119 (1), 151–162. doi:10.1002/2013JA019269
- Zou, Y., Nishimura, Y., Lyons, L. R., Shiokawa, K., Donovan, E. F., Ruohoniemi, J. M., et al. (2015). Localized polar cap flow enhancement tracing using airglow patches: Statistical properties, IMF dependence, and contribution to polar cap convection. *J. Geophys. Res. Space Phys.* 120, 4064–4078. doi:10.1002/2014JA020946